Trans. of the Society of Instrument and Control Engineers
Vol.E2, No.1, 108/114 (2002)

Control of Nonlinear Hysteresis Systems by Riemannian Geometric Approach†

Yoshiaki IZAWA* and Kyojiro HAKOMORI*

This paper presents a designing method for nonlinear systems that have hysteresis properties in the input stage. The hysteresis properties are usually described by two-valued nonlinear functions. Therefore it is more difficult to design the nonlinear hysteresis systems.

By using the idea of topology, we consider first how to represent such a hysteresis property as a one-valued function. To this modified nonlinear system, we construct a Riemannian geometric nonlinear optimal regulator that has been proposed by the authors. Because the nonlinear geometric regulator is homeomorphic to a linear optimal regulator, the superior properties of a linear regulator (i.e., asymptotic stability, feedback construction and so on) are also reflected in the nonlinear regulator.

As an example, the temperature control system with a bimetal thermal sensor is investigated.

Key Words: hysteresis, nonlinear system, optimal regulator, Riemannian geometric approach, gauge field

1. Introduction

Some of the real plants have the non-negligible hysteresis properties. These properties are appeared especially in the thermal systems controlled by bimetal thermal sensors, hydraulic servo systems controlled by on-off valves with clatter properties, high accuracy position control systems by piezo actuators and so on. Since the hysteresis systems are described by two-valued nonlinear functions and often bring the limit cycles [1], many control designers feel great difficulties.

In this paper we first represent the nonlinear systems without two-valued functions by the idea of topology. Next, we design these systems by the Riemannian geometric approach [2), 3)] proposed by authors. In this theory we have derived a nonlinear optimal regulator whose topological structure is equivalent to that of an appropriate paired linear regulator. Last, we investigate the control performance through the numerical examples of a temperature control with a bimetal thermal sensor.

2. Geometrical Interpretation of Hysteresis and Designing Principle

In topological geometry, the torus T^2 shown in **Fig. 1** is interpreted as a manifold which is homeomorphic to the 2-dimensional Euclidean space constructed by the direct product $S^1 \times S^1$ of two circumferences.

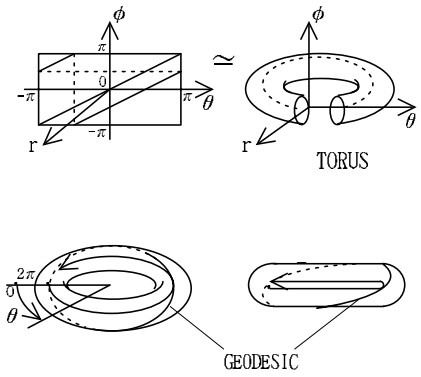

Fig. 1 Geometric interpretation of hysteresis

Therefore a closed geodesic on a torus is appeared as a line on the above 2-dimensional Euclidean space and represented by 1 parameter θ.

When the torus is looked at sideways (i.e., looked from hole-less direction) and mapped to a plane, the closed geodesic is mapped as an ellipse. This ellipse is usually represented by a two-valued function. On the other hand, the ellipse can be also described by a one-valued function of 1 parameter θ, because the ellipse is derived from a closed geodesic. The same discussion leads that the hysteresis properties can be represented by one-valued functions of 1 parameter θ.

Now, we assume that the input block $b(u)$ shown in **Fig. 2** has a hysteresis property composed by an ellipse (i.e., closed geodesic).

† Received the SICE best paper award of 1999

* Department of Mechanical Engineering, Tohoku University, Aramaki, Sendai, 980-0845, Japan

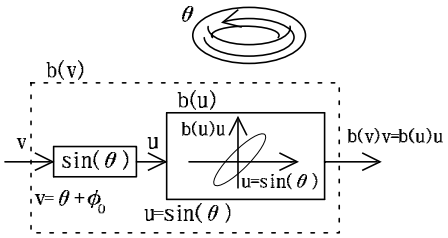

Fig. 2 Representation of a two-valued hysteresis function with 1 parameter θ

Consider a system input u and a fictitious input v or θ defined as following equations.

$$u = \sin(\theta) \tag{1}$$

$$v = \theta + \phi_0 \qquad (-\pi \ < \ \phi_0 \ < \ 0) \tag{2}$$

Here v has a phase lag ϕ_0 behind θ.
Because the output signal of the dotted fictitious block $b(v)$ in Fig. 2 is equivalent to that of the input block $b(u)$, we have the following relation.

$$b(v)v = b(u)u \tag{3}$$

Since the hysteresis property of $b(u)$ is given as an ellipse and can be regarded as a special pattern of Lissajous' figures made from two sine functions whose phases are different from each other, we have

$$b(u) = \frac{\sin(\theta+\phi_0)}{\sin(\theta)} = \frac{\sin(\sin^{-1}(u)+\phi_0)}{u}, \tag{4}$$

$$-\pi \ < \ \phi_0 \ < \ 0. \tag{5}$$

We will now confirm that the above $b(u)$ becomes a two-valued function of u. The function $\sin^{-1}(u)$ involved in a numerator takes the following values with respect to the points A and B in **Fig. 3**.

$$\sin^{-1}(u) = \begin{cases} 2n\pi + \theta & (\text{ to point } A\ ) \\ (2n+1)\pi - \theta & (\text{ to point } B\ ) \end{cases} \tag{6}$$

$$(n = 0,\ \pm 1,\ \pm 2,\ \ldots) \tag{7}$$

Therefore $\sin^{-1}(u)$ is represented as a multi-valued function of the input u $(-1 \le u \le 1)$.
Let the point A' and B' have a same phase lag ϕ_0 behind points A and B each other. Then the numerator of (4), i.e., $f \equiv \sin(\sin^{-1}(u)+\phi_0)$, is given as the following values with respect to points A' and B'.

$$\sin(\sin^{-1}(u)+\phi_0) = \begin{cases} f_{A'} \\ f_{B'} \end{cases} \tag{8}$$

Thus the function $b(u)$ defined in (4) becomes a two-valued function of u. However, $b(u)$ defined in (4) can be interpreted simultaneously as a one-valued function with respect to θ, because both numerator and denominator of (4) are one-valued functions with respect to θ .

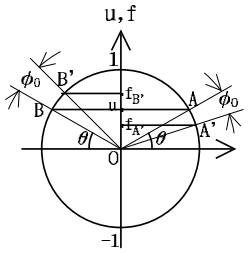

Fig. 3 Illustration of $f = \sin\{\sin^{-1}(u) + \phi_0\}$

Consider the function $b(v)$ of a fictitious input v. Substituting (4) and (1) into (3), and considering (2), we have

$$b(v) = \sin(v)\ /v \tag{9}$$

Therefore the hysteresis property defined by $b(v)$ is represented as a one-valued function with respect to a fictitious input v.

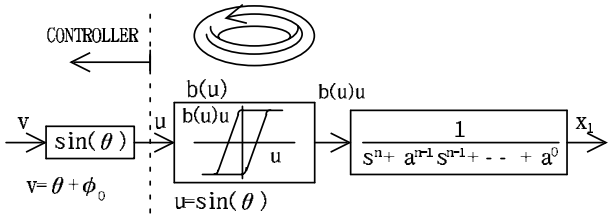

Fig. 4 One input imaginary system which represents the hysteresis property with 1 parameter θ

Now, consider a one-input hysteresis system shown in **Fig. 4**. Regarding the hysteresis property as a deformation of the ellipse defined in Fig. 2, the system equation is given as

$$\begin{pmatrix} \dot{x_1} \\ \vdots \\ \dot{x_n} \end{pmatrix} = \begin{pmatrix} 0 & 1 & 0 & \cdots & 0 \\ 0 & 0 & 1 & \cdots & 0 \\ & & & \ddots & \\ 0 & 0 & \cdots & 0 & 1 \\ -a^0 & -a^1 & \cdots & \cdots & -a^{n-1} \end{pmatrix} \begin{pmatrix} x_1 \\ \vdots \\ x_n \end{pmatrix} + \begin{pmatrix} 0 \\ \cdots \\ 0 \\ b(v) \end{pmatrix} v, \tag{10}$$

$$b(v) = k \cdot \tanh(h \cdot \sin(v))\ /v. \tag{11}$$

Here $b(v)$ is a one-valued nonlinear function of a fictitious input v.

On the other hand, the hysteresis system of Fig. 4 can be represented by using a real input u. From (10), (11) and the following relation

$$v = \sin^{-1}(u) + \phi_0, \tag{12}$$

we have

$$\begin{pmatrix} \dot{x_1} \\ \vdots \\ \dot{x_n} \end{pmatrix} = \begin{pmatrix} 0 & 1 & 0 & \cdots & 0 \\ 0 & 0 & 1 & \cdots & 0 \\ & & & \ddots & \\ 0 & 0 & \cdots & 0 & 1 \\ -a^0 & -a^1 & \cdots & \cdots & -a^{n-1} \end{pmatrix} \begin{pmatrix} x_1 \\ \vdots \\ x_n \end{pmatrix} + \begin{pmatrix} 0 \\ \cdots \\ 0 \\ b(u) \end{pmatrix} u, \tag{13}$$

$$b(u) = k \cdot \tanh(h \cdot \sin(\sin^{-1}(u) + \phi_0)) \ /u. \tag{14}$$

Here $b(u)$ becomes a two-valued function of u .

Thus we have shown the procedure to represent the hysteresis property as a one-valued nonlinear function by introducing a fictitious input v. In later sections, we will construct a nonlinear optimal regulator by adopting the hysteresis system (10) with v instead of the system (13) with u. Then the real input u will be given by using the fictitious optimal control v_{opt} as

$$u = \sin(v_{opt} - \phi_0). \tag{15}$$

3. Riemannian Geometric Approach [2), 3)]

In this section a Riemannian geometric nonlinear optimal regulator is constructed by the following idea.

" When the trajectories of a linear system is observed on a set of curvilinear coordinate axes instead of the orthogonal straight coordinate axes, then the trajectories behave like a nonlinear system. Conversely, the trajectories of a nonlinear system can be treated as those of a linear system by using a suitable set of curvilinear coordinate axes."

Consider a nonlinear system (16) and its paired fictitious linear system (17).

$$\dot{x} = a(x, v)x + b(x, v)v, \tag{16}$$

$$\dot{X} = AX + BV. \tag{17}$$

Here x, X are n-dimensional vectors, v, V are r-dimensional vectors, $a(x, v), A$ are $n \times n$ matrixes, and $b(x, v), B$ are $n \times r$ matrixes.

Let $\tilde{\mathcal{X}}, \bar{\mathcal{X}}$ be (n + r)-dimensional vectors spanned on a direct product space of the state vector space and the control vector space.

$$\tilde{\mathcal{X}} = \begin{pmatrix} x \\ v \end{pmatrix}, \qquad \bar{\mathcal{X}} = \begin{pmatrix} X \\ V \end{pmatrix}. \tag{18}$$

Then (16), (17) are given as

$$\dot{\tilde{\mathcal{X}}} = \tilde{\alpha}(\tilde{\mathcal{X}})\ \tilde{\mathcal{X}}, \ \ \tilde{\alpha}(\tilde{\mathcal{X}}) = \begin{pmatrix} a(x,v) & b(x,v) \\ 0 & 0 \end{pmatrix}. \tag{19}$$

$$\dot{\bar{\mathcal{X}}} = \bar{\mathcal{A}}\ \bar{\mathcal{X}}, \qquad \bar{\mathcal{A}} = \begin{pmatrix} A & B \\ 0 & 0 \end{pmatrix}. \tag{20}$$

Tensor representations of these equations (19), (20) will lead the following Riemannian geometric models.

Now, let $\tilde{\mathcal{X}}^\mu$, $\tilde{\mathcal{A}}^\mu_\nu$ be tensors described on the curvilinear coordinate system $(\tilde{x}^i)$, $i = 1, \cdots, n + r$. And let $\bar{\mathcal{X}}^\mu, \bar{\mathcal{A}}^\mu_\nu$ be their paired tensors described on the orthogonal straight coordinate system $(\bar{x}^i)$. Then the components of these tensors are transferred as

$$\bar{\mathcal{X}}^\mu = \frac{\partial \bar{x}^\mu}{\partial \tilde{x}^\gamma}\ \tilde{\mathcal{X}}^\gamma, \tag{21}$$

$$\bar{\mathcal{A}}^\mu_\nu = \frac{\partial \bar{x}^\mu}{\partial \tilde{x}^\alpha}\frac{\partial \tilde{x}^\beta}{\partial \bar{x}^\nu}\ \tilde{\mathcal{A}}^\alpha_\beta. \tag{22}$$

According to the matrix representation of tensors [2), 3)], a contravariant vector is expressed as a column vector, and (1,1)-tensor $\mathcal{T}^\mu_\nu$ is expressed as a matrix with (μ, ν) element $\mathcal{T}^\mu_\nu$. Therefore a linear system (20) is represented as a tensor equation

$$\frac{d}{dt}\bar{\mathcal{X}}^\mu = \bar{\mathcal{A}}^\mu_\nu\ \bar{\mathcal{X}}^\nu. \tag{23}$$

Substituting (21) into (23), we have

$$\frac{\partial \bar{x}^\mu}{\partial \tilde{x}^\gamma}\frac{d\tilde{\mathcal{X}}^\gamma}{dt} + \frac{\partial^2 \bar{x}^\mu}{\partial \tilde{x}^\beta \partial \tilde{x}^\lambda}\frac{d\tilde{x}^\lambda}{dt}\ \tilde{\mathcal{X}}^\beta = \bar{\mathcal{A}}^\mu_\nu \frac{\partial \bar{x}^\nu}{\partial \tilde{x}^\rho}\ \tilde{\mathcal{X}}^\rho. \tag{24}$$

Multiplying $\frac{\partial \tilde{x}^\gamma}{\partial \bar{x}^\mu}$ into (24), we have

$$\frac{d\tilde{\mathcal{X}}^\gamma}{dt} + \frac{\partial \tilde{x}^\gamma}{\partial \bar{x}^\mu}\frac{\partial^2 \bar{x}^\mu}{\partial \tilde{x}^\beta \partial \tilde{x}^\lambda}\frac{d\tilde{x}^\lambda}{dt}\tilde{\mathcal{X}}^\beta = \frac{\partial \tilde{x}^\gamma}{\partial \bar{x}^\mu}\ \bar{\mathcal{A}}^\mu_\nu\ \frac{\partial \bar{x}^\nu}{\partial \tilde{x}^\rho}\ \tilde{\mathcal{X}}^\rho. \tag{25}$$

Using (22) and the Christoffel symbols defined as

$$\widetilde{\{^\nu_{\lambda\mu}\}} = \frac{1}{2}g^{\nu k}\left(\frac{\partial g_{\lambda k}}{\partial \tilde{x}^\mu} + \frac{\partial g_{k\mu}}{\partial \tilde{x}^\lambda} - \frac{\partial g_{\mu\lambda}}{\partial \tilde{x}^k}\right) = \frac{\partial \tilde{x}^\nu}{\partial \bar{x}^i}\frac{\partial^2 \bar{x}^i}{\partial \tilde{x}^\lambda \partial \tilde{x}^\mu}, \tag{26}$$

where $g_{\mu\nu}$ is a metric tensor, (25) becomes

$$\frac{d\tilde{\mathcal{X}}^\gamma}{dt} + \widetilde{\{^\gamma_{\beta\lambda}\}}\frac{d\tilde{x}^\lambda}{dt}\tilde{\mathcal{X}}^\beta = \tilde{\mathcal{A}}^\gamma_\rho\ \tilde{\mathcal{X}}^\rho. \tag{27}$$

Theorem 1. The linear system (23) described on the orthogonal straight coordinate system $(\bar{x}^i), i = 1, \ldots, n + r$, is represented on the curvilinear coordinate system $(\tilde{x}^i)$ as the equation (27).

Proof. Proof is given as above. Q.E.D.

This Riemannian geometric model has a dual model.

Theorem 2. The transposed linear system

$$\frac{d\bar{\mathcal{X}}_\mu}{dt} = \bar{\mathcal{X}}_\nu \ {}^t\overline{\mathcal{A}}^\nu_\mu \tag{28}$$

described on the orthogonal straight coordinate system $(\bar{x}^i),\ i = 1, \ldots, n+r$, is represented on the curvilinear coordinate system $(\tilde{x}^i)$ as

$$\frac{d\tilde{\mathcal{X}}_\rho}{dt} - \tilde{\mathcal{X}}_\beta \frac{d\tilde{x}^\delta}{dt}\widetilde{\{^\beta_{\delta\rho}\}} = \tilde{\mathcal{X}}_\beta \ \widetilde{{}^t\mathcal{A}^\beta_\rho}. \tag{29}$$

Proof. See *Theorem* 2 in Ref. 3). Q.E.D.

Using the Riemannian metric tensor $g_{\mu\nu}$, the following relation holds good between the contravariant and covariant vectors $\tilde{\mathcal{X}}^\nu,\ \tilde{\mathcal{X}}_\mu$ in *Theorem* 1, 2.

$$\tilde{\mathcal{X}}_\mu = g_{\mu\nu}\tilde{\mathcal{X}}^\nu \tag{30}$$

And the tensor ${}^t\mathcal{A}^\nu_\mu$ has the following properties.

$$\overline{{}^t\mathcal{A}}^i_j = \bar{\mathcal{A}}^j_i \tag{31}$$

Consider the mapping between two integral manifolds of the Riemannian geometric model on the orthogonal straight coordinate system and the curvilinear coordinate system. Let $\tau^\nu_\gamma,\ \mathcal{T}^\gamma_\nu$ be

$$\tau^\nu_\gamma = \frac{\partial\bar{x}^\nu}{\partial\tilde{x}^\gamma}, \quad \mathcal{T}^\gamma_\nu = \frac{\partial\tilde{x}^\gamma}{\partial\bar{x}^\nu}.$$

Then the transformation formulas of tensor components

$$\bar{\mathcal{X}}^\nu = \frac{\partial\bar{x}^\nu}{\partial\tilde{x}^\gamma}\ \tilde{\mathcal{X}}^\gamma, \tag{32}$$

$$\bar{\mathcal{X}}_\nu = \frac{\partial\tilde{x}^\gamma}{\partial\bar{x}^\nu}\ \tilde{\mathcal{X}}_\gamma \tag{33}$$

can be regarded as the mappings between $\bar{\mathcal{X}}^\nu$ and $\tilde{\mathcal{X}}^\gamma$ using τ and $\mathcal{T}$. If both τ and $\mathcal{T}$ are continuous mappings, then the mapping τ becomes the homeomorphism between two integral manifolds.

Using these τ and $\mathcal{T}$, the Riemannian geometric model (27) and its dual model (29) become

$$\frac{d\tilde{\mathcal{X}}^\gamma}{dt} = (\mathcal{T}^\gamma_\mu\bar{\mathcal{A}}^\mu_\nu\tau^\nu_\rho - \mathcal{T}^\gamma_\mu\frac{d\tau^\mu_\rho}{dt})\ \tilde{\mathcal{X}}^\rho, \tag{34}$$

$$\frac{d\tilde{\mathcal{X}}_\rho}{dt} = \tilde{\mathcal{X}}_\beta(\mathcal{T}^\beta_\nu\overline{{}^t\mathcal{A}}^\nu_\mu\tau^\mu_\rho - \frac{d\mathcal{T}^\beta_\mu}{dt}\tau^\mu_\rho). \tag{35}$$

Thus the following Riemannian geometric nonlinear optimal regulator is derived.

Theorem 3. When the homeomorphism τ exists and is represented as

$$\left(\tau^i_j\right) = \begin{matrix} \\ n \\ r \end{matrix}\begin{matrix} \begin{matrix} n & r \end{matrix} \\ \begin{pmatrix} \tau_{11} & \tau_{12} \\ \tau_{21} & \tau_{22} \end{pmatrix} \end{matrix}, \tag{36}$$

then for the Riemannian geometric model (27) or (34) and the performance index

$$J = \frac{1}{2}\int_{t_0}^{T} \tilde{\mathcal{X}}_i\mathcal{T}^i_\nu\bar{\mathcal{Q}}^\nu_\mu\tau^\mu_j\tilde{\mathcal{X}}^j\ dt \tag{37}$$

$$\left(\bar{\mathcal{Q}}^\nu_\mu\right) = \begin{matrix} \\ n \\ r \end{matrix}\begin{matrix} \begin{matrix} n & r \end{matrix} \\ \begin{pmatrix} Q & 0 \\ 0 & R \end{pmatrix} \end{matrix}, \tag{38}$$

where $\bar{\mathcal{Q}}^\nu_\mu$ is positive definite, we have the optimal control law

$$v = -(\tau_{22} + K\tau_{12})^{-1}(\tau_{21} + K\tau_{11})x \tag{39}$$

$$K = R^{-1}B^tS. \tag{40}$$

Here S is the solution of the Riccati equation

$$\frac{dS}{dt} + SA + A^tS - SBR^{-1}B^tS + Q = 0, \tag{41}$$

$$S(T) = 0. \tag{42}$$

Proof. See *Theorem* 3 in Ref. 3). Q.E.D.

Next we consider the infinite-time nonlinear regulator problem.

Theorem 4. When the homeomorphism τ exists, the fictitious linear system (20) or (23) is completely controllable and the matrix representations of $\left(\tau^i_j\right),\ \left(\bar{\mathcal{Q}}^\nu_\mu\right)$ are given as (36), (38) respectively, then for the Riemannian geometric model (27) or (34) and the performance index

$$J = \frac{1}{2}\int_{t_0}^{\infty} \tilde{\mathcal{X}}_i\mathcal{T}^i_\nu\bar{\mathcal{Q}}^\nu_\mu\tau^\mu_j\tilde{\mathcal{X}}^j\ dt, \tag{43}$$

where $\bar{\mathcal{Q}}^\nu_\mu$ is positive definite, we have the optimal control law

$$v = -(\tau_{22} + K\tau_{12})^{-1}(\tau_{21} + K\tau_{11})x, \tag{44}$$

$$K = R^{-1}B^tS. \tag{45}$$

Here S is the solution of the algebraic Riccati equation

$$SA + A^tS - SBR^{-1}B^tS + Q = 0. \tag{46}$$

Proof. The Riccati equation derived in *Theorem* 3 is equivalent to that of a finite-time linear optimal regulator and does not depend on the homeomorphism τ. Furthermore, in *Theorem* 6 shown later, the homeomorphism τ is only determined by the equality between the Riemannian geometric model and the nonlinear system. Therefore, the construction problem of τ is independent of the optimal problem. Thus the finite-time nonlinear optimal problem in *Theorem* 3 can be separated into the finite-time linear optimal regulator problem for a fictitious linear system and the construction problem of τ.

Similarly, the infinite-time nonlinear regulator problem which is the special case of the finite-time problem can also be separated into the infinite-time linear regulator problem and the construction problem of τ.

Consequently, Kalman's discussion constructing a infinite-time linear regulator for a completely controllable linear system is acceptable (see Chap.6 in Ref. 4)). Thus the solution S of the Riccati equation (41) becomes a constant matrix and we have (46). Q.E.D.

Theorem 5. Nonlinear regulator given in *Theorem* 4 is asymptotic stable [5].

Proof. See *Theorem* 4 in Ref. 3). Now the asymptotic stability [5] is only defined in the case of an infinite time interval ($T \to \infty$). Q.E.D.

Next, we consider the construction method of the curvilinear coordinate system on which the nonlinear system

$$\frac{d\tilde{\mathcal{X}}^{\gamma}}{dt} = \tilde{\alpha}^{\gamma}_{\mu}(\tilde{\mathcal{X}})\ \tilde{\mathcal{X}}^{\mu} \tag{47}$$

is observed as a linear system (23).

Since the equation (47) is equivalent to the Riemannian geometric model (27), we have

$$\tilde{\mathcal{A}}^{\gamma}_{\mu} - \widetilde{\{_{\mu}{}^{\gamma}{}_{\lambda}\}}\frac{d\tilde{x}^{\lambda}}{dt} = \tilde{\alpha}^{\gamma}_{\mu}(\tilde{\mathcal{X}}). \tag{48}$$

Using (22) and the relations

$$\widetilde{\{_{\mu}{}^{\gamma}{}_{\lambda}\}} = \mathcal{T}^{\gamma}_{\beta}\frac{\partial \tau^{\beta}_{\mu}}{\partial \tilde{x}^{\lambda}}, \tag{49}$$

$$\frac{\partial \tau^{\beta}_{\mu}}{\partial \tilde{x}^{\lambda}}\frac{d\tilde{x}^{\lambda}}{dt} = \frac{d\tau^{\beta}_{\mu}}{dt} = \frac{\partial \tau^{\beta}_{\mu}}{\partial \tilde{\mathcal{X}}^{\lambda}}\frac{d\tilde{\mathcal{X}}^{\lambda}}{dt}, \tag{50}$$

the equation (48) becomes the following partial differential equation with respect to τ.

$$\frac{\partial \tau^{\beta}_{\mu}}{\partial \tilde{\mathcal{X}}^{\lambda}}[\tilde{\alpha}^{\lambda}_{\gamma}(\tilde{\mathcal{X}})\ \tilde{\mathcal{X}}^{\gamma}] = \bar{\mathcal{A}}^{\beta}_{\nu}\tau^{\nu}_{\mu} - \tau^{\beta}_{\gamma}\,\tilde{\alpha}^{\gamma}_{\mu}(\tilde{\mathcal{X}}) \tag{51}$$

Theorem 6. The homeomorphism τ between the integral manifold of a nonlinear system (19) and that of a linear system (20) satisfies a partial differential equation (51).

Proof. Proof is given as above. Q.E.D.

Since the equation (51) is a quasi-linear partial differential equation of first order, we have the following characteristic equations.

$$\frac{d\tilde{\mathcal{X}}^{\gamma}}{dt} = \tilde{\alpha}^{\gamma}_{\mu}(\tilde{\mathcal{X}})\ \tilde{\mathcal{X}}^{\mu} \tag{52}$$

$$\frac{d\tau^{\beta}_{\mu}}{dt} = \bar{\mathcal{A}}^{\beta}_{\nu}\tau^{\nu}_{\mu} - \tau^{\beta}_{\gamma}\,\tilde{\alpha}^{\gamma}_{\mu}(\tilde{\mathcal{X}}). \tag{53}$$

The nonlinear optimal regulator derived in *Theorem* 4 is realized by using the algorithm in Ref. 2).

4. Control of Nonlinear Hysteresis System

This section presents a designing method for nonlinear hysteresis systems.

First, we consider the nonlinear hysteresis system (10) with a fictitious input v. Second, we construct a nonlinear optimal regulator based on Theorem 4 and derive v_{opt}. Last, a real input u is given as

$$u = \sin(v_{opt} - \phi_0). \tag{54}$$

The flow chart is shown in **Fig. 5**.

< Numerical Example >

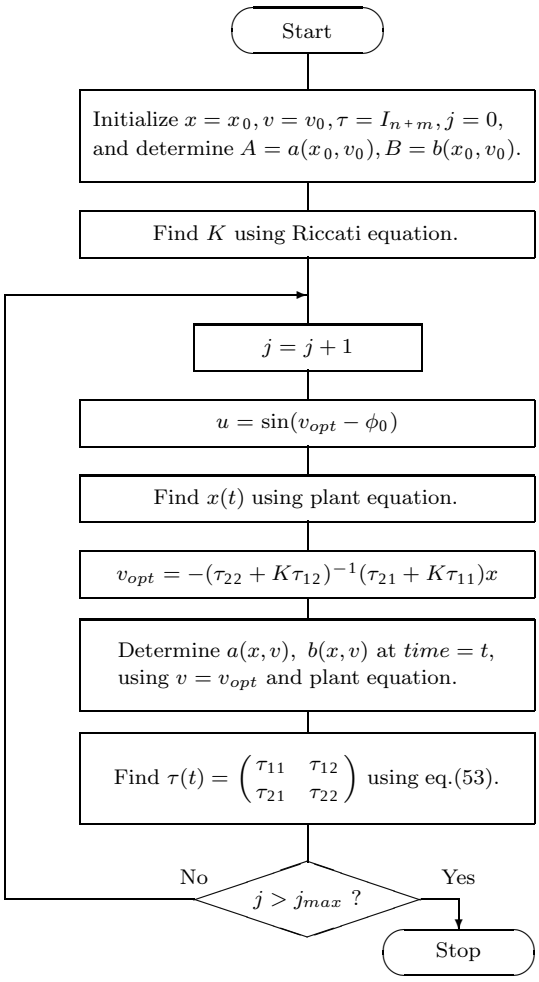

Fig. 5 Flow chart for designing the nonlinear hysteresis system

Consider the temperature control [1] of the compartment in an airplane shown in **Fig. 6**.

The heat from electric devices is detected by the bimetal

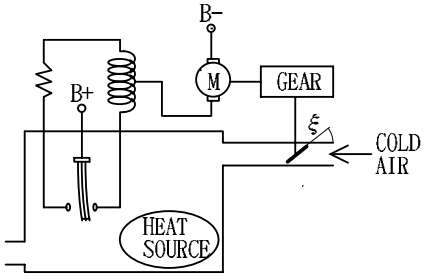

Fig. 6 Temperature control of a compartment with bimetal thermal sensor

thermal sensor. When the temperature in the compartment rises, the current flowing to the DC motor increases in the opposite direction and the inlet valve is opened. These control operations lead the temperature constant.

The bimetal switch has a hysteresis property shown in **Fig. 7**. Here Θ is the temperature of a compartment, and ξ, $\dot{\xi}$ are the revolution angle and its derivative of an inlet valve, respectively.

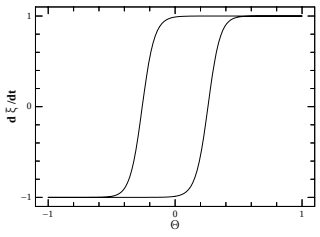

Fig. 7 Hysteresis of an inlet valve ($\phi_0 = -15°, h = 10.0$)

Table 1 System variables of the temperature control system

System variables	
M	mass of compartment
C	specific heat
S	closs area of compartment
α	thermal conductivity
Θ	temperature of compartment
q	heat

The system variables are shown in **Table 1**. Considering the heat balance, the system equation is derived as

$$M\ C\ d\Theta\ +\ S\ \alpha\ \Theta\ dt\ =\ \dot{q}\ dt. \tag{55}$$

Since the heat inflow from the outside depends on the position of a inlet valve, the heat variation $\dot{q}$ is given as

$$\dot{q}\ =\ -\ K\ \xi(\Theta)\ +\ f(t),\quad K > 0 \tag{56}$$

$$\dot{f}(t)\ =\ 0. \tag{57}$$

Thus we have

$$T_1\ \dot{\Theta} + \Theta\ =\ -\ K_1\ \xi(\Theta)\ +\ f_1(t), \tag{58}$$

where

$$T_1 = \frac{M\ C}{S\ \alpha},\quad K_1 = \frac{K}{S\ \alpha},\quad f_1(t) = \frac{f(t)}{S\ \alpha}. \tag{59}$$

Differentiating (58) with time, we have

$$T_1\ \ddot{\Theta} + \dot{\Theta} + K_1\ \dot{\xi}(\Theta) = 0. \tag{60}$$

The bimetal switch is working as a temperature sensor and an on-off switch. **Fig. 8** is a simulation system in which the on-off switch is replaced by a relay with a hysteresis property. Let e be an input voltage of the relay, and $\xi_1(e)$ be a revolution angle of the inlet valve with respect to the input voltage e. Then the hysteresis property is represented as

$$\dot{\xi}_1(e) = \dot{\xi}(\Theta). \tag{61}$$

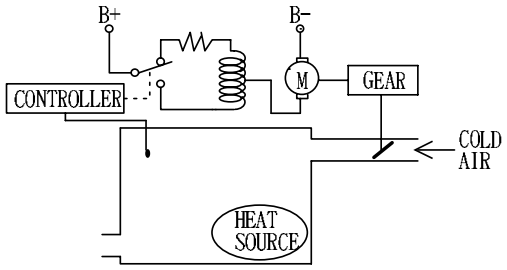

Fig. 8 Temperature control of the compartment with thermal sensor and relay

Using the state and control vectors $x_1 = \Theta$, $x_2 = \dot{\Theta}$, $u = e$, and considering (60), (61), the system equation of Fig. 8 is derived as

$$\frac{d}{dt}\begin{pmatrix} x_1 \\ x_2 \end{pmatrix} = \begin{pmatrix} 0 & 1 \\ 0 & -\frac{1}{T_1} \end{pmatrix}\begin{pmatrix} x_1 \\ x_2 \end{pmatrix} + \begin{pmatrix} 0 \\ -\frac{K_1}{T_1}\dot{\xi}_1(u)\ /\ u \end{pmatrix} u. \tag{62}$$

Here the hysteresis function $\dot{\xi}_1(u)$ is given as

$$\dot{\xi}_1(u)\ =\ \tanh(h \cdot \sin(v)), \tag{63}$$

$$v\ =\ \sin^{-1}(u) + \phi_0. \tag{64}$$

To investigate the characteristic property of this system, we consider the following approximate linear system.

$$\frac{d}{dt}\begin{pmatrix} x_1 \\ x_2 \end{pmatrix} = \begin{pmatrix} 0 & 1 \\ 0 & -\frac{1}{T_1} \end{pmatrix}\begin{pmatrix} x_1 \\ x_2 \end{pmatrix} + \begin{pmatrix} 0 \\ -\frac{K_1}{T_1}h \end{pmatrix} u. \tag{65}$$

The transfer function is given as

$$G(s) = \frac{-K_1 h}{(T_1 s + 1)s}. \tag{66}$$

Considering a PID-control $u = -(k_p x_1 + k_i \int x_1 dt + k_d \frac{dx_1}{dt})$, the Hurwitz stability conditions are given as

$$k_p < 0,\ k_i < 0,\ k_d < \frac{1}{K_1 h}(1 - \frac{T_1 k_i}{k_p}). \tag{67}$$

In the case of $K_1 = 1.0$, $T_1 = 1.0$, $\phi_0 = -15°$, $h = 10.0$, the simulation results are shown in **Fig. 9** ($k_p = -0.5$, $k_i = -0.2$, $k_d = -0.1$) and **Fig. 10** ($k_p = -5.0$, $k_i = -2.0$, $k_d = -0.05$).

Here dotted lines, long-dotted lines and solid lines show $x_1(t)$, $x_2(t)$ and $u(t)$, respectively. The desired values are given as $x_1 = x_2 = 0$. In both cases, the stability conditions are satisfied. Although Fig. 9 shows good responses, Fig. 10 shows an unstable case with a limit cycle.

The simulation results of our nonlinear regulators are shown in **Fig. 11** and **Fig. 12**. Here $Q = I_2$, $R = I_1$, and the step widths of time are $\Delta = 0.01$.

The meanings of lines are as above and one dotted lines show $v(t)$. The difference between Fig. 11 and Fig. 12 is

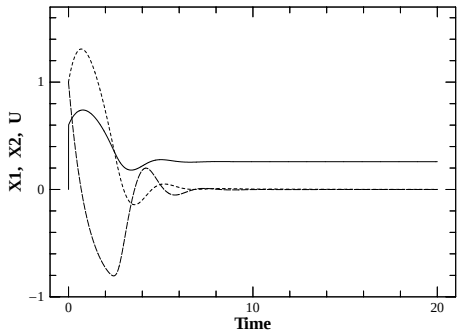

Fig. 9 Responses of the temperature control system with PID-control ($k_p = -0.5,\ k_i = -0.2,\ k_d = -0.1$)

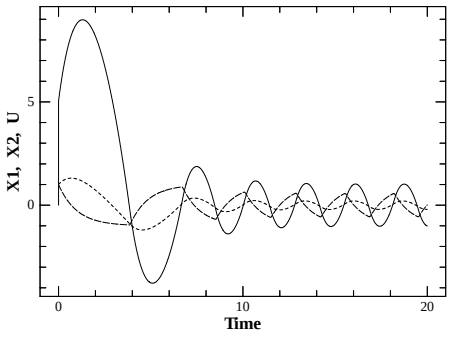

Fig. 10 Responses of the temperature control system with PID-control ($k_p = -5.0,\ k_i = -2.0,\ k_d = -0.05$)

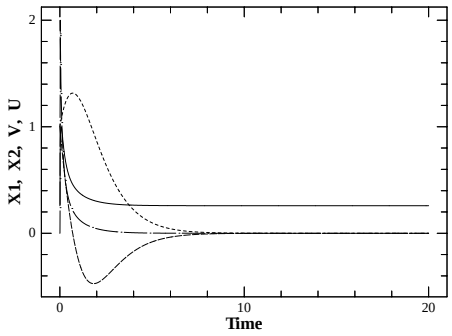

Fig. 11 Responses of the temperature control system with nonlinear regulator (case-1)

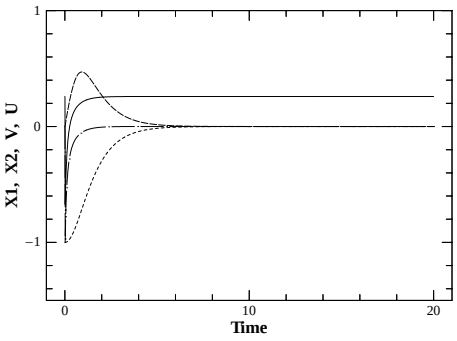

Fig. 12 Responses of the temperature control system with nonlinear regulator (case-2)

only in the initial conditions.

5. Conclusions

The designing methods of nonlinear hysteresis systems have been proposed. In section 2, the hysteresis system has been described with a one-valued function by considering the closed geodesic on a torus. In section 3, the nonlinear optimal regulator has been introduced by using Riemannian geometry. In section 4, the example for a thermal hysteresis system has been shown, and the usefulness of this approach has been confirmed.

References

1) J.E.Gibson: Nonlinear Automatic Control, McGraw-Hill (1963)
2) Y.Izawa and K.Hakomori: Design of Nonlinear Regulators Using Riemannian Geometric Model, SICE Trans., **16**-5, 628/634 (1980)
3) Y.Izawa and K.Hakomori: Nonlinear Control of a Double-Effect Evaporator by Riemannian Geometric Approach, SICE Trans., **32**-2, 197/206 (1996)
4) R.E.Kalman: Contribution to the theory of optimal control, Bol. Soc. Mat. Mexicana, Vol. **5**, 102/119 (1960)
5) J.LaSalle and S.Lefschetz: Stability by Lyapunov's Direct Method with Applications, Academic Press (1961)

Yoshiaki Izawa (Member)

He was born in 1948. He received the Dr. Eng. degree in Precision Engineering from Tohoku University, in 1980. From 1981 to 2000, he was a Research Associate and an Assistant Professor of Department of Mechanical Engineering, Tohoku University. Currently, he has left from Tohoku University. His research interests are in the nonlinear system theories and their applications.

Kyojiro Hakomori (Member)

He received the D. E. degree in Precision Engineering from Tohoku University, Japan, in 1962. From 1962 to 1996, he was an Assistant Professor, an Associate Professor and a Professor of Department of Mechanical Engineering, Tohoku University. Since 1996, he has been a Professor of Tohoku Gakuin University. His research interests include measurement and control theory, and robotics.

Reprinted from Trans. of the SICE
Vol.33 No.12 1124/1130 1997